基于Lyapunov控制方法的量子C–NOT门的实现

NOURALLAH Ghaeminezhad[1], 丛 爽[1†], 双 丰[2]
(1. 中国科学技术大学 自动化系, 安徽 合肥 230027; 2. 中国科学院 智能机械研究所, 安徽 合肥 230031)

摘要: 本文研究了量子C–NOT门的制备. Cartan分解和Lyapunov控制方法用于设计实现C–NOT门的两个量子位操作的控制手段. 数值仿真实验表明, 针对所设计的控制律, 若给定合适的控制参数, 每个单量子比特旋转在所考虑的轴周围具有较小的偏差, 并且在1.68 a.u.

关键词: C–NOT门; Cartan分解; Lyapunov控制方法
引用格式: NOURALLAH Ghaeminezhad, 丛爽, 双丰. 基于Lyapunov控制方法的量子C–NOT门的实现. 控制理论与应用, 2019, 36(8): 1296 – 1303
DOI: 10.7641/CTA.2019.18075

Realization of quantum C–NOT gates based on the Lyapunov control method

NOURALLAH Ghaeminezhad[1], CONG Shuang[1†], SHUANG Feng[2]
(1. Department of Automation, University of Science and Technology of China, Hefei Anhui 230027, China;
2. Institute of Intelligent Machines, Chinese Academy of Sciences, Hefei Anhui 230031, China)

Abstract: The preparation of the quantum C–NOT gate is studied in this paper. The Cartan decomposition and the Lyapunov control methods are used to design the control laws for two single-qubit operations in realizing the C–NOT gate. The numerical simulation experiments show that for some proper control parameters in the designed control laws, each single qubit rotation has less deviation around the considered axis, and the total Fidelity of the system can achieve to 1, after 1.68 a.u..

Key words: C–NOT gate; Cartan decomposition; Lyapunov control method
Citation: NOURALLAH Ghaeminezhad, CONG Shuang, SHUANG Feng. Realization of quantum C–NOT gates based on the Lyapunov control method. *Control Theory & Applications*, 2019, 36(8): 1296 – 1303

1 Introduction

The quantum computing is a major area of interesting in the field of quantum computation, in which the quantum computers will perform much faster than current classical computers and will open a new view point to many aspects of science. The two qubit C–NOT gate is an important component in the quantum circuits, and it combines some single qubit operation to realize any quantum computation. Therefore, it plays a key role in developing the quantum computers[1–3]. One of the most important events in the field of quantum computation and information happened in 1970 s, when the control over single quantum system was completely obtained[4]. Recent developments in quantum control have heightened the need for solid-state systems, in which the state of electron confined in the semiconductor quantum dots can be manipulated[5–9]. A considerable amount of literatures have been published on the realization of coupled qubits, among them there have been a number of longitudinal studies involving the decomposition methods, in which the Cartan decomposition is an increasingly important method used to realize the quantum gates[10–18]. However, in the methods mentioned above, the centered axis of the rotation in each single-qubit operation of the decomposed step has not been investigated; therefore the Fidelity of the system could not reach to 1.

The Lyapunov control method is one of the most widely used methods of controlling quantum states and has been extensively used for theoretical and experimental researches[19–24].

The purpose of this paper is to realize the two qubit

Received 4 April 2018; Accepted 18 January 2019.
†Corresponding author. E-mail: scong@ustc.edu.cn; Tel.: +86 551-63600710.
Recommended by Associate Editor: SHI Guo-dong.
Supported by the National Natural Science Foundation of China (61573330), the National Natural Science Foundation of International (Regional) Cooperation and Exchanges Project (61720106009) and the Chinese Academy of Sciences (CAS) and the World Academy of Sciences (TWAS).

C–NOT gate by manipulating the quantum dot system in order to achieve a high Fidelity in a short time. A combination of the Cartan decomposition method and the Lyapunov control method is used to design the control laws in each decomposed step. The control task is to reduce the rotation swing and achieve higher Fidelity in a short time, while preparing the two qubit C–NOT gate.

The rest of the paper is arranged as follows: Section 2 is the model description of the research and defines the system Hamiltonian. Section 3 is concerned with the Canonical decomposition and realization process of C–NOT gate. Section 4 gives the design of the Lyapunov control laws. Section 5 is the numerical experiments and result discussion. Finally, the conclusion gives a brief summary of the proposed work.

2 Description of the model

Quantum dots are made from semiconductor materials, metals, or small molecules, in which the electric charge spins are confined and can be manipulated by applying pulsed local electromagnetic fields to operate the single qubit rotations[25].

A quantum system with single-spin has two states, i.e., $\psi_0 = \begin{pmatrix}1\\0\end{pmatrix}$ and $\psi_1 = \begin{pmatrix}0\\1\end{pmatrix}$, which are represented as $|0\rangle$ and $|1\rangle$, respectively. The superposition principle in quantum theory yields that, any state of the single-spin system can be described as $\psi = a\psi_0 + b\psi_1$, where $|a|^2 + |b|^2 = 1$ and $a,\ b \in \mathbb{C}$, in which $\mathbb{C}$ denotes the set of complex numbers[26].

In this paper, we deal with the two-spin (two quantum-dots) system, so the Hilbert space is the tensor product of each single-spin space, and accordingly there are 4 eigenstates as

$$\{|0\rangle\otimes|0\rangle, |0\rangle\otimes|1\rangle, |1\rangle\otimes|0\rangle, |1\rangle\otimes|1\rangle\} = \{[1\ 0\ 0\ 0]^{\mathrm{T}},\ [0\ 1\ 0\ 0]^{\mathrm{T}},\ [0\ 0\ 1\ 0]^{\mathrm{T}},\ [0\ 0\ 0\ 1]^{\mathrm{T}}\}. \quad (1)$$

The underlying Hilbert space of the system is

$$H = \mathrm{span}\,\{|00\rangle, |01\rangle, |10\rangle, |11\rangle\}. \quad (2)$$

The wave function $|\psi(\mathrm{t})\rangle$ of the system has four components:

$$|\psi(\mathrm{t})\rangle = \mathrm{a}_1|00\rangle + \mathrm{a}_2|01\rangle + \mathrm{a}_3|10\rangle + \mathrm{a}_4|11\rangle, \quad (3)$$

in which $|\psi(\mathrm{t})\rangle$ satisfies the Schrödinger equation

$$\begin{cases} i\hbar\dfrac{\partial}{\partial t}|\psi\,(t)\rangle = H(t)|\psi\,(t)\rangle, \ \ t>0, \\ |\psi(0)\rangle = |\psi_0\rangle \in \mathcal{H}, \end{cases} \quad (4)$$

where, $\mathcal{H}$ denotes the Hilbert space, and $H(t)$ is the total Hamiltonian of the system.

According to the Hubbard model, the total Hamiltonian of a two quantum-dots system in the interaction picture can be written as [27]:

$$H = \sum_{i=1}^{2}\frac{\hbar}{2}\mu_{\mathrm{B}} g_i(t) B_i(t)\cdot S_i + \frac{\hbar}{2}J_{12}(t) S_1\cdot S_2, \quad (5)$$

where, the μ_{B} is the Bohr magneton; $g_i(t)$ is the effective g-factor; $B_i, i = 1, 2$ is the number of applied magnetic fields to the electron spin at dot i in the directions of x, y or z, and $J_{12}(t)$ is the time-dependent coupling component between quantum dots 1 and 2.

In (5), S_1 and S_2 are the spin operators for the first and second quantum dots, respectively. By defining the Pauli spin vector which has matrix components, we have

$$S_1 = \sigma = (\sigma_{\mathrm{x}}\ \ \sigma_{\mathrm{y}}\ \ \sigma_{\mathrm{z}})^{\mathrm{T}} = \sigma_{\mathrm{x}}e_{\mathrm{x}} + \sigma_{\mathrm{y}}e_{\mathrm{y}} + \sigma_{\mathrm{z}}e_{\mathrm{z}} \quad (6)$$

and

$$S_2 = \tau = (\tau_{\mathrm{x}},\ \ \tau_{\mathrm{y}}\ \ \tau_{\mathrm{z}})^{\mathrm{T}} = \tau_{\mathrm{x}}e_{\mathrm{x}} + \tau_{\mathrm{y}}e_{\mathrm{y}} + \tau_{\mathrm{z}}e_{\mathrm{z}}, \quad (7)$$

where $\sigma_{\mathrm{x}}, \sigma_{\mathrm{y}}, \sigma_{\mathrm{z}}$ and $\tau_{\mathrm{x}}, \tau_{\mathrm{y}}, \tau_{\mathrm{z}}$ are the usual Pauli matrices of the first and second qubits, respectively; $e_{\mathrm{x}}, e_{\mathrm{y}}$ and e_{z} are the unit vectors in directions of x, y and z:

$$\begin{cases} \sigma_{\mathrm{x}} = \tau_{\mathrm{x}} = \begin{bmatrix}0 & 1\\ 1 & 0\end{bmatrix},\ \sigma_{\mathrm{y}} = \tau_{\mathrm{y}} = \begin{bmatrix}0 & -i\\ i & 0\end{bmatrix}, \\ \sigma_{\mathrm{z}} = \tau_{\mathrm{z}} = \begin{bmatrix}1 & 0\\ 0 & -1\end{bmatrix}. \end{cases} \quad (8)$$

Based on (5), we define the control laws $\Omega_i(t) = \mu_{\mathrm{B}} g_i(t) B_i(t), i = 1, 2$. These are applied to the first and second qubits, respectively. The coupling component between two qubits is defined as $\omega(t) = J_{12}(t)$. Therefore, the total Hamiltonian of the system consists of control (external) Hamiltonian $H_{\mathrm{c}}(t)$ and interaction Hamiltonian $H_{\mathrm{I}}(t)$:

$$H(t) = \frac{\hbar}{2}[(\Omega_1(t)(\sigma\otimes \boldsymbol{I}) + \Omega_2(t)(\boldsymbol{I}\otimes\tau)) + \omega(t)(\sigma\otimes\tau)],$$
$$H(t) = H_{\mathrm{c}}(t) + H_{\mathrm{I}}, \quad (9)$$

where, $\boldsymbol{I}$ is a 2×2 identity matrix operator that sets the Hilbert space of Hamiltonian as a 4×4 matrix. This is used to show there is no interaction between qubits in the first and second terms. The σ and τ are two Pauli matrices related to the first and second qubit, respectively; and $\sigma\tau$ is the tensor product between them:

$$\begin{cases} \sigma\tau = \sigma\otimes\tau = \sigma_{\mathrm{x}}\otimes\tau_{\mathrm{x}} + \sigma_{\mathrm{y}}\otimes\tau_{\mathrm{y}} + \sigma_{\mathrm{z}}\otimes\tau_{\mathrm{z}}, \\ \sigma\boldsymbol{I} = \sigma\otimes\boldsymbol{I} = \sigma_{\mathrm{x}}\otimes\boldsymbol{I} + \sigma_{\mathrm{y}}\otimes\boldsymbol{I} + \sigma_{\mathrm{z}}\otimes\boldsymbol{I}, \\ \boldsymbol{I}\tau = \boldsymbol{I}\otimes\tau = \boldsymbol{I}\otimes\tau_{\mathrm{x}} + \boldsymbol{I}\otimes\tau_{\mathrm{y}} + \boldsymbol{I}\otimes\tau_{\mathrm{z}}. \end{cases} \quad (10)$$

We set the Plank constant $\hbar = 1$ for the simplicity. The Ising interaction is considered for 2-qubit coupling interaction, so we have the effect of entangler part only along the z-axis, then the system Hamiltonian is

$$H(t) = H_{\Omega_1}(t) + H_{\Omega_2}(t) + H_{\omega}(t) = \frac{1}{2}[\Omega_1(t)\sigma\boldsymbol{I} + \Omega_2(t)\boldsymbol{I}\tau + \omega(t)\sigma_{\mathrm{z}}\tau_{\mathrm{z}}]. \quad (11)$$

3 Analysis of quantum C–NOT gate via Cartan decomposition

3.1 Canonical decomposition of the unitary gate

Generally speaking, the unitary time-evolution operator $U(t)$ can be used to drive the system from any initial state to the target state. If the Hamiltonian of the system is time dependent, given the state at some initial time ($t = 0$), we can solve the Schrödinger (4) to obtain the state at any subsequent time as

$$\big|\psi\,(t)\big\rangle = \mathrm{e}^{-i\int_0^T H(t)\mathrm{d}t/\hbar}\big|\psi\,(0)\big\rangle = U(t)\big|\psi\,(0)\big\rangle. \tag{12}$$

We define $u^k_{\Omega_i(t)}(\theta), k = x, y, z,\ i = 1$, (2) as the unitary evolution operator that makes -2θ rotation along the related pauli matrix $\sigma_k, \tau_k, k = x, y, z$; for the first (or second) qubit. As it was mentioned in (11) the total Hamiltonian of the two-qubit system consists of 3 parts, therefore, the total unitary time-evolution operator $U(t)$ consists of 3 parts as well:

1) Let $u^k_{\Omega_1(t)}(\theta), k = x, y, z$; be the unitary evolution on the first qubit where the pulses are chosen such that: $\omega(t) = \Omega_2(t) = 0$; while for the scalar valued $\Omega_1(t)$:

$$\int_0^T \Omega_1(t)\mathrm{d}t = 2\theta,\ t\ \in\ [0,\ T\,]. \tag{13}$$

According to (11) we have

$$H_{\Omega_1}(t) = \frac{1}{2}\Omega_1(t)\sigma\boldsymbol{I}, \tag{14}$$

$$u^k_{\Omega_1(t)}(\theta) = \mathrm{e}^{-\frac{i}{2}\int_0^T H_{\Omega_1}(t)\mathrm{d}t} =$$
$$\mathrm{e}^{-\frac{i}{2}\int_0^T \Omega_1(t)\sigma_k\boldsymbol{I}\mathrm{d}t} = \mathrm{e}^{[-\frac{i}{2}\int_0^T \Omega_1(t)\mathrm{d}t]\sigma_k\boldsymbol{I}} =$$
$$\mathrm{e}^{-i\theta\sigma_k\boldsymbol{I}} = \cos\theta\boldsymbol{I} - i\sin\theta\sigma_k\boldsymbol{I};\ k = x, y, z, \tag{15}$$

where I is a 4 by 4 identity matrix.

2) To define the $u^k_{\Omega_2(t)}(\theta)$ for second qubit, we set $\Omega_1(t) = \omega(t) = 0$, where

$$\int_0^T \Omega_2(t)\mathrm{d}t = 2\theta,\ t \in [0, T]. \tag{16}$$

Based on (11) and (12) the Hamiltonian of second qubit and the unitary evolution are defined as:

$$H_{\Omega_2}(t) = \frac{1}{2}\Omega_2(t)\boldsymbol{I}\tau, \tag{17}$$

$$u^k_{\Omega_2(t)}(\theta) = \mathrm{e}^{-\frac{i}{2}\int_0^T H_{\Omega_2}(t)\mathrm{d}t} =$$
$$\mathrm{e}^{-\frac{i}{2}\int_0^T \Omega_2(t)\ \boldsymbol{I}\tau_k\mathrm{d}t} = \mathrm{e}^{[-\frac{i}{2}\int_0^T \Omega_2(t)\mathrm{d}t\ ]\boldsymbol{I}\tau_k} =$$
$$\mathrm{e}^{-i\theta\boldsymbol{I}\tau_k} = \cos\theta\ \boldsymbol{I} - i\sin\theta\boldsymbol{I}\tau_k,\ k = x, y, z. \tag{18}$$

3) The evolution of the entangler part (A_ω), evolves under the interaction picture by defining the fixed coupling component $\omega(t) = \pi$, during the 0.5 a.u. interval of time evolution, i.e. $t_2 - t_1 = 0.5$ a.u.:

$$\int_{t_1}^{t_2} \omega(t)\mathrm{d}t = \frac{\pi}{2},\ t_1, t_2 \in [0, T]. \tag{19}$$

Referring to (11) and (12) we have

$$H_\omega(t) = \frac{\omega(t)}{2}\sigma_{\mathrm{z}}\tau_{\mathrm{z}}, \tag{20}$$

$$A_\omega = \mathrm{e}^{-i\int_{t_1}^{t_2} H_\omega(t)\mathrm{d}t/\hbar} = \mathrm{e}^{i\frac{\pi}{4}\sigma_{\mathrm{z}}\tau_{\mathrm{z}}} =$$
$$\cos\frac{\pi}{4}\boldsymbol{I} + i\sin\frac{\pi}{4}\sigma_{\mathrm{z}}\tau_{\mathrm{z}}. \tag{21}$$

3.2 Realization process of the C–NOT gate by Cartan decomposition

According to the Cartan decomposition[14] for the Controlled-NOT operation, the unitary time-evolution operator $U_{\mathrm{C-NOT}}$ can be represented by the following sequence of magnetic-field pulses (which make the local rotations) and nonlocal entangler part:

$$U_t = \mathrm{e}^{i\frac{\pi}{4}} \cdot U^{\mathrm{z}}_{\Omega_1(t)}(-\frac{\pi}{4}) \cdot U^{\mathrm{y}}_{\Omega_2(t)}(\frac{\pi}{4}) \cdot$$
$$U^{\mathrm{z}}_{\Omega_2(t)}(\frac{\pi}{4}) \cdot A_\omega \cdot U^{\mathrm{y}}_{\Omega_2(t)}(-\frac{\pi}{4}), \tag{22}$$

in which, each time sequence of operations from right to left are defined as, $U_{t_i},\ i = 0, \cdots, 6$; and they are shown in Fig. 1, where $U_{t_0} = U_0 = I$, is the initial gate, and $U_{t_6} = U_{\mathrm{f}} = U_{\mathrm{C-NOT}}$ is the final C–NOT gate. We recall that an operator $u^k_{\Omega_i(\theta)}(t),\ k = x, y, z,\ i = 1$ (or 2); corresponds to an operation on the first (or second) qubit in the Bloch vector space, that makes a rotation around the axis k by angle -2θ.

The C–NOT gate flips the second (target) qubit if the first (control) qubit is in the state $|1\rangle$. In the completion of evaluating the U_t in (22), the process of preparing the C–NOT gate is carried out by taking the $U_{t_0} = I$, as the initial gate:

1) The first operation, $U^{\mathrm{y}}_{\Omega_2(t)}(-\frac{\pi}{4})$, rotates the second qubit $|\psi_2\rangle$ by $+90^\circ$ about the y axis, i.e., the state $|1\rangle$ in the second qubit is rotated from $-z$ to $-x$. According to Fig. 1 and (18) we have the U_{t_1} as

$$U_{t_1} = U^{\mathrm{y}}_{\Omega_{01}(t)}(-\frac{\pi}{4}) \cdot U_{t_0} = \mathrm{e}^{-i\frac{\pi}{4}\tau_{\mathrm{y}}} \cdot U_{t_0} =$$
$$\frac{1}{\sqrt{2}}\begin{bmatrix}1&-1&0&0\\1&1&0&0\\0&0&1&-1\\0&0&1&1\end{bmatrix}\begin{bmatrix}1&0&0&0\\0&1&0&0\\0&0&1&0\\0&0&0&1\end{bmatrix} = \frac{1}{\sqrt{2}}\begin{bmatrix}1&-1&0&0\\1&1&0&0\\0&0&1&-1\\0&0&1&1\end{bmatrix}. \tag{23}$$

2) The second operation, A_ω, implies a conditional rotation. It rotates qubit 2 by $+90^\circ$ around the $\hat{z}$ axis if qubit 1 is $|0\rangle$, but it rotates qubit 2 by -90° around the $\hat{z}$ axis if qubit 1 is $|1\rangle$. Based on Fig. 1 and (21) the U_{t_2} is

$$U_{t_2} = A_\omega \cdot U_{t_1} = \mathrm{e}^{-i\frac{\pi}{4}\sigma_{\mathrm{z}}\tau_{\mathrm{z}}} \cdot U_{t_1} =$$
$$\frac{1}{\sqrt{2}} \cdot \begin{bmatrix}1-i&0&0&0\\0&1+i&0&0\\0&0&1+i&0\\0&0&0&1-i\end{bmatrix}.$$

$$\frac{1}{\sqrt{2}}\cdot\begin{bmatrix}1&-1&0&0\\1&1&0&0\\0&0&1&-1\\0&0&1&1\end{bmatrix}=$$

$$\frac{1}{2}\cdot\begin{bmatrix}1-i&i-1&0&0\\1+i&1+i&0&0\\0&0&1+i&-1-i\\0&0&1-i&1-i\end{bmatrix}. \tag{24}$$

3) The third operation, $U^{\mathrm{z}}_{\Omega_2(t)}(\frac{\pi}{4})$, rotates qubit 2 by -90° around the $\hat{z}$ axis:

$$U_{t_3}=U^{\mathrm{z}}_{\Omega_{23}(t)}(\frac{\pi}{4})\cdot U_{t_2}=\mathrm{e}^{i\frac{\pi}{4}\tau_{\mathrm{z}}}\cdot U_{t_2}=$$

$$\frac{1}{\sqrt{2}}\cdot\begin{bmatrix}1+i&0&0&0\\0&1-i&0&0\\0&0&1+i&0\\0&0&0&1-i\end{bmatrix}\cdot\frac{1}{2}\cdot$$

$$\begin{bmatrix}1-i&i-1&0&0\\1+i&1+i&0&0\\0&0&1+i&-1-i\\0&0&1-i&1-i\end{bmatrix}=$$

$$\frac{1}{\sqrt{2}}\cdot\begin{bmatrix}1&-1&0&0\\1&1&0&0\\0&0&i&-i\\0&0&-i&-i\end{bmatrix}. \tag{25}$$

4) The fourth operation, $U^{\mathrm{y}}_{\Omega_{34}(t)}(\frac{\pi}{4})$, rotates qubit 2 by -90° around the $\hat{y}$ axis which brings back the qubit 2 to its first origin state if qubit 1 is $|0\rangle$, but flips qubit 2 in the case the state of qubit 1 is $|1\rangle$:

$$U_{t_4}=U^{\mathrm{y}}_{\Omega_{34}(t)}(\frac{\pi}{4})\cdot U_{t_3}=\mathrm{e}^{i\frac{\pi}{4}\tau_{\mathrm{y}}}\cdot U_{t_3}=$$

$$\frac{1}{\sqrt{2}}\cdot\begin{bmatrix}1&1&0&0\\-1&1&0&0\\0&0&1&1\\0&0&-1&1\end{bmatrix}\cdot\frac{1}{\sqrt{2}}\cdot\begin{bmatrix}1&-1&0&0\\1&1&0&0\\0&0&i&-i\\0&0&-i&-i\end{bmatrix}=$$

$$\begin{bmatrix}1&0&0&0\\0&1&0&0\\0&0&0&-i\\0&0&-i&0\end{bmatrix}. \tag{26}$$

Step 4 completes the realization of the C–NOT gate, and the next step is to tiding up the phases of qubits in the case when qubit 1 is not in the basis states.

In (26) the global phase shift $-i$, does not have any effect on the evolution, and the C–NOT gate is realized in this step, therefore, it is decided to ignore steps 5 and 6 during the next sections, where the control laws are designed and experimental simulation are done.

5) The fifth operation $U^{\mathrm{z}}_{\Omega_1(t)}(-\frac{\pi}{4})$, rotates qubit 1 by $+90^\circ$ around the $\hat{z}$ axis to tide up the phases of the qubits. According to Fig. 1 and (15) one has

$$U_{t_5}=U^{\mathrm{z}}_{\Omega_{45}(t)}(-\frac{\pi}{4})\cdot U_{t_4}=\mathrm{e}^{i\frac{\pi}{4}\tau_{\mathrm{y}}}\cdot U_{t_4}=$$

$$\frac{1}{\sqrt{2}}\cdot\begin{bmatrix}1-i&0&0&0\\0&1-i&0&0\\0&0&1+i&0\\0&0&0&1+i\end{bmatrix}\cdot\begin{bmatrix}1&0&0&0\\0&1&0&0\\0&0&0&-i\\0&0&-i&0\end{bmatrix}=$$

$$\frac{1}{\sqrt{2}}\cdot\begin{bmatrix}1-i&0&0&0\\0&1-i&0&0\\0&0&0&1-i\\0&0&1-i&0\end{bmatrix}. \tag{27}$$

6) This operation implies a phase shift $\mathrm{e}^{i\frac{\pi}{4}}$ on U_{t_5}:

$$U_{t_{\mathrm{f}}}=\mathrm{e}^{i\frac{\pi}{4}}\cdot U_{t_5}=\frac{1+i}{\sqrt{2}}\cdot U_{t_5}=$$

$$\frac{1+i}{\sqrt{2}}\cdot\frac{1}{\sqrt{2}}\cdot\begin{bmatrix}1-i&0&0&0\\0&1-i&0&0\\0&0&0&1-i\\0&0&1-i&0\end{bmatrix}=\begin{bmatrix}1&0&0&0\\0&1&0&0\\0&0&0&1\\0&0&1&0\end{bmatrix}. \tag{28}$$

The output of this step shows the whole process is equal to the C–NOT gate operation.

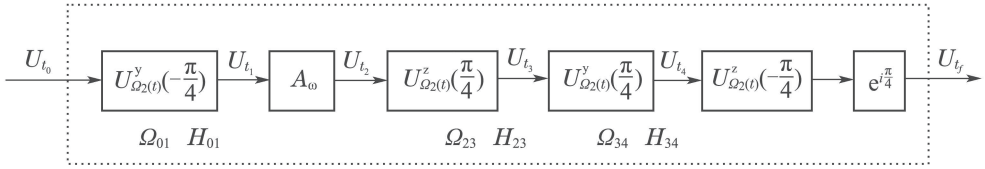

Fig. 1 The realization process schematic diagram. It should be noted that the control pulse $\Omega_2(t)$ is implemented locallyand separately to the second qubit, in different time sequences and based to the corresponding Hamiltonian H. Regard to Fig. 1 and (11), as $\Omega_2(t)$ is applied to the second qubit in the times t_0, t_2 and t_3, it is re-named as Ω_{01}, Ω_{23} and Ω_{34} and the related Hamiltonians are: $H_{01}=H_{34}=\frac{1}{2}\boldsymbol{I}\tau_{\mathrm{y}}$ and $H_{23}=\frac{1}{2}\boldsymbol{I}\tau_{\mathrm{z}}$. To drive U_{t_1} to U_{t_2}, the evolution goes under interaction Hamiltonian by selecting the proper coupling component $\omega(t)$ during entangler part A_ω

4 Design of Lyapunov control laws

The control method used in this paper is based on the Lyapunov control method. The Lyapunov control method has showed the better ability to provide efficient control laws that act fantastic for the gate preparing and designing the control laws. The main idea of the Lya-

punov control method is to design a proper function $V(x)$ with the two following conditions along any time of evolution: 1) $V(x)$ must be semi-positive definite, i.e., $V(x) \geqslant 0, \forall x \in \mathbb{R}$, where R denotes the set of real numbers. 2) The first derivative of $V(x)$ is always semi-negative definite, i.e., $\dot{V}(x) \leqslant 0,\ \forall x \in \mathbb{R}$[26].

In this Section, the purpose of designing the Lyapunov control laws is to drive the U_{t_0} to U_{t_f} as shown in Fig. 1. We let each column of unitary time-evolution operator be representative of the state vector as

$$\begin{cases} U_{t_0} = \begin{bmatrix} \psi_{0_{11}} & \psi_{0_{21}} & \psi_{0_{31}} & \psi_{0_{41}} \\ \psi_{0_{12}} & \psi_{0_{22}} & \psi_{0_{32}} & \psi_{0_{42}} \\ \psi_{0_{13}} & \psi_{0_{23}} & \psi_{0_{33}} & \psi_{0_{43}} \\ \psi_{0_{14}} & \psi_{0_{24}} & \psi_{0_{34}} & \psi_{0_{44}} \end{bmatrix} = \\ [|\psi_{0_1}\rangle\ |\psi_{0_2}\rangle\ |\psi_{0_3}\rangle\ |\psi_{0_4}\rangle], \\ U_{t_\mathrm{f}} = [|\psi_{\mathrm{f}_1}\rangle\ |\psi_{\mathrm{f}_2}\rangle\ |\psi_{\mathrm{f}_3}\rangle\ |\psi_{\mathrm{f}_4}\rangle]. \end{cases} \tag{29}$$

Based on the Schrödinger equation in (4), the evolution of the wave function in (12), and the evolution of the C–NOT gate in (22), the realization of the C–NOT gate is to design the control laws Ω, which imply to each columns of U_{t_0} and drive them to the final C–NOT gate U_{t_f} at the same time:

$$|\psi_{f_i}\rangle = U_t \cdot |\psi_{0_i}\rangle,\ i = 1, 2, 3, 4, \tag{30}$$

where U_t is defined in (22), and as the phase shift $-i$ in (26) is ignored in this paper, the evolution during experiment is up to step 4 of Fig. 1.

In this paper during the evolution, all the designing process of Lyapunov function is carried out by using the real parts of the state elements, therefore, in terms of $|\psi\rangle = [x_1 + ix_5\ \ x_2 + ix_6\ \ x_3 + ix_7\ \ x_4 + ix_8]^{\mathrm{T}}$, we consider $|x\rangle = [x_1\ x_2\ x_3\ x_4\ x_5\ x_6\ x_7\ x_8]^{\mathrm{T}}$ as the real valued state which has more convenient mathematical calculations.

By adapting the state $|x\rangle$ with the Schrödinger (4), we can see that the real and imaginary part on each side are equal, respectively, therefore, we have

$$\dot{x}(t) = B\Omega(t)x(t). \tag{31}$$

where, $B = \begin{bmatrix} I(H) & R(H) \\ -R(H) & I \end{bmatrix}$ is the skew symmetric matrix in which each element stands for imaginary (I) or real (R) part of the total Hamiltonian $H(t)$ in (11).

During the whole derivation process, the (31) can be allocated to each step of Fig. 1 as

$$\dot{x}_{t_{i,i+1}}(t) = B_{i,i+1}\Omega_{i,i+1}(t)x_{t_i}(t),\ i = 0, 2, 3, \tag{32}$$

where

$$B_{i,i+1} = \begin{bmatrix} I(H_{i,i+1}) & R(H_{i,i+1}) \\ -R(H_{i,i+1}) & I(H_{i,i+1}) \end{bmatrix},\ i = 0, 2, 3,$$

and

$$H_{01} = H_{34} = \frac{1}{2}\boldsymbol{I}\tau_{\mathrm{y}} = \begin{bmatrix} 0 & -i & 0 & 0 \\ i & 0 & 0 & 0 \\ 0 & 0 & 0 & -i \\ 0 & 0 & i & 0 \end{bmatrix},$$

$$H_{23} = \frac{1}{2}\boldsymbol{I}\tau_{\mathrm{z}} = \begin{bmatrix} 1 & 0 & 0 & 0 \\ 0 & -1 & 0 & 0 \\ 0 & 0 & 1 & 0 \\ 0 & 0 & 0 & -1 \end{bmatrix}.$$

The general form of the Lyapunov function for the system (31) is constructed as follows:

$$V(x) = \frac{1}{2} \cdot (x - x_{\mathrm{f}})^{\mathrm{T}} P (x - x_{\mathrm{f}}), \tag{33}$$

where according to (32), for each step of Fig. 1 we have

$$V_{i,i+1}(x) = \frac{1}{2} \cdot (x_{t_{i,i+1}} - x_{t_{i+1}})^{\mathrm{T}} P (x_{t_{i,i+1}} - x_{t_{i+1}}),\ i = 0, 2, 3, \tag{34}$$

while P is an arbitrary semi-positive definite symmetric matrix, that makes the Lyapunov function $V(x)$ be semi-positive for all amount of x, which is the satisfaction of the first condition of the Lyapunov control method, i.e., $V_i(x) > 0, \forall x \in \mathbb{R}$ and $V_{i,i+1}(x) = 0$ when $|x_{t_{i,i+1}}\rangle = |x_{t_{i+1}}\rangle,\ i = 0, 2, 3$.

The first order time derivative of $V_{i,i+1}(x)$ is

$$\dot{V}_{i,i+1}(x) = (x_{t_{i,i+1}} - x_{t_{i+1}})^{\mathrm{T}} P \dot{x}_{t_{i,i+1}},\ i = 0, 2, 3. \tag{35}$$

Substituting (32) into (35) we have $\dot{V}(x)$ as

$$\dot{V}_{i,i+1}(x) = (x_{t_{i,i+1}} - x_{t_{i+1}})^{\mathrm{T}} P B_{i,i+1} \Omega_{i,i+1}(t) x_{t_{i,i+1}},\ i = 0, 2, 3. \tag{36}$$

To meet the second condition of the Lyapunov control method, the control laws must be designed in such a way that $\dot{V}(t) \leqslant 0,\ \forall t \in \mathbb{R}$. The constructed control laws are

$$\Omega_{i,i+1}(t) = -k_{i,\,i+1}(x_{t_i} - x_{t_{i+1}})^{\mathrm{T}} P B_{i,i+1} x_{t_i} k_{i,i+1} > 0,\ i = 0, 2, 3. \tag{37}$$

Substituting (37) into (36):

$$\dot{V}_{i,i+1}(x) = -k_{i,\,i+1}[(x_{t_{i,i+1}} - x_{t_{i+1}})^{\mathrm{T}} P B_{i,i+1} x_{t_{i,i+1}}]^2 \leqslant 0,\ i = 0, 2, 3, \tag{38}$$

which means, by using the designed control laws $\dot{V}_{i,i+1}(x) < 0, \forall x \in \mathbb{R}$, and $\dot{V}_{i,i+1}(x) = 0$ when $|x_{t_{i,i+1}}\rangle = |x_{t_{i+1}}\rangle,\ i = 0, 2, 3$.

After obtaining the requirements of the Lyapunov control method, in the next section the experiments are done by using the control laws designed in (37), where

$B_{i,i+1}$, $i = 0, 2, 3$ are defined as mentioned in (32), $P = \mathrm{diag}\{[1, 2, 1, 2, 1, 2, 1, 2]\}$ is a semi-positive definite symmetric matrix, and $k_{i,\,i+1}$, $i = 0, 2, 3$ are the control parameters, which are chosen during the experiment.

5 Numerical experiments and result discussions

In this Section, the experimental results of unitary time-evolution is illustrated. The effect of control laws is to drive the initial gate, U_{t_0}, to achieve the desired gate U_{t_f}, according to related decomposed steps of Fig. 1. According to (29) and (30), in order to drive U_{t_0} to U_{t_f}, the designed control laws in (37) are implemented simultaneously to each columns (states) of U_{t_0}, through the each decomposed step. Considering the columns of U_{t_0} in (29) as the initial states, Fig. 2 illustrates the *X*–*Y* and *Y*–*Z* plane trajectories, after applying the unitary evolution operators of (23)–(26) on second qubit, when the designed control laws of (37) are implemented to the system for different groups of control parameters, k_1, k_3 and k_4. It must be mentioned that during the step 2 of evolution the system goes under the interaction picture, in which coupling constant $\omega(t) = J_{I2}(t) = \pi$, therefore, there is no effect of control laws.

In Figs. 2(a) and 2(b), by implementing and adjusting the control parameters of the designed control laws in (37), i.e., $K_i (i = 1, 3, 4)$, the plane trajectories of *X*–*Y* and *Y*–*Z* are compared during different steps.

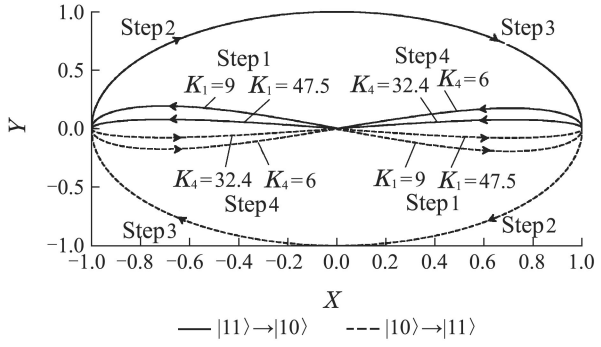

(a)

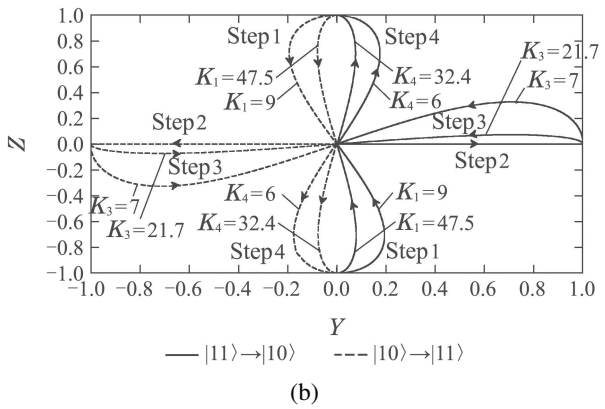

(b)

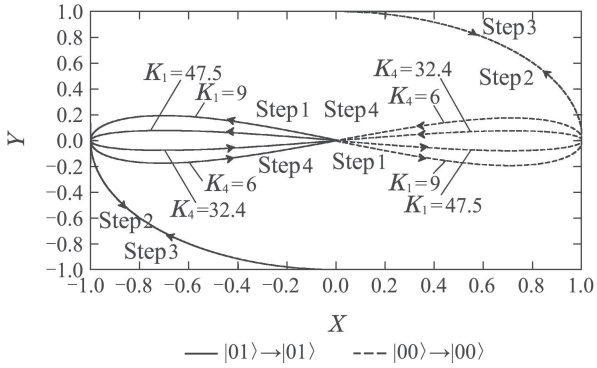

(c)

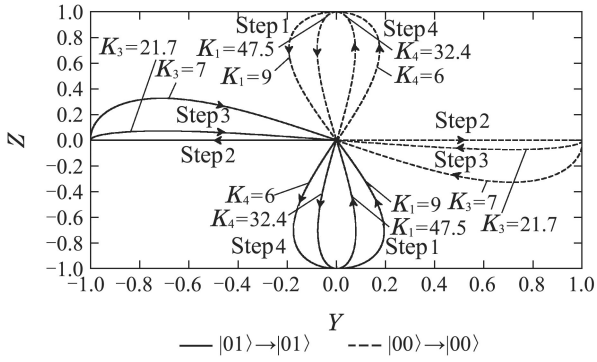

(d)

Fig. 2 Trajectory of state evolution shown in *X*–*Y* and *Y*–*Z* plane

According to Fig. 2 and (23)–(26), the operation of the first step rotates the second qubit by $+90^\circ$ around the y axis, therefore when the initial state is $|11\rangle$ the value of *X* goes from 0 to -1 and the value of *Z* changes from -1 to 0. Similarly when the initial state is $|10\rangle$, *X* and *Z* change from 0 and 1 to 1 and 0, respectively. In Step 2, fixed value of $\omega(t)$ is used to drive *X* from -1 to 0, and *Y* from 0 to 1, when the initial state is $|11\rangle$. For the initial state $|10\rangle$ the changing trends are from 1 to 0 and from 0 to -1, for *X* and *Y*, respectively. In Step 3, where there is a rotation about -90° around the $\hat{z}$ axis, the *X* and *Y* values change from 0 to 1 and from 1 to 0 for the initial state $|11\rangle$, and for the initial state $|10\rangle$ these trends are from 0 to -1 and -1 to 0 for *X* and *Y*, respectively. Following the process of evolution, in response to the operation of step 4 for $|11\rangle$ as the initial state, the values of *X* and *Z* move from 1 and 0 to 0 and 1, respectively; while these trends are from -1 and 0 to 0 and -1, for $|10\rangle$ as the initial state.

Similarly, the Figs. 2(c) and 2(d) provide the intercorrelations among the 4-steps evolution of *X*, *Y* and *Z*, in which for the $|01\rangle$, and $|00\rangle$ as the initial states, the values of *X*, *Y* and *Z* return to their initial amount, because the C–NOT gate does not change the second qubit when the first qubit is $|0\rangle$. In Fig. 2, When the *X*–*Y* and *Y*–*Z* planes are plotted separately, it can be seen that the evolution has deviation from the rotation trajectory around the fixed axis. A possible explanation for these

results may be the intrinsic errors which are caused by weak driving of applied magnetic field, $B_j(t)$, and assuming fixed coupling between the qubits through the evolution. The first and forth steps of experiment, emphasize the impact of control laws in rotation. By using different control parameters K_1 and K_4 in *X–Y* and *Y–Z* plane, the deviation of *Y* component is reduced.

Assessing the evolution of Step 3 the similar-behavior can be seen by using the different control parameter K_3, when the *Z* component deviates from zero in *Y–Z* plane. For the first group of control parameters, i.e., $K_1 = 9$, $K_3 = 7$, and $K_4 = 6$, there are a 0.32 deviation from rotation trajectory around the centered axis. However, following the procedure of evolution, by using the designed control laws in (37) and adjusting different control parameters, it is apparent that for the second group of control parameters, i.e., $K_1 = 47.5$, $K_3 = 21.7$ and $K_4 = 32.4$, the *Y* and *Z* components remain close to zero and have only deviation about 0.091.

Once the proper control parameters are adjusted, the probability evolutions of each state element in U_{t_0}, i.e., $|\psi_{0_{11}}|^2$ to $|\psi_{0_{44}}|^2$ are shown in Fig. 3 when the initial states are $|11\rangle$, $|10\rangle$, $|01\rangle$ and $|00\rangle$, respectively. The results as shown in Fig. 3, indicate that by simultaneous implementing of the designed control laws in (37) to each column of identity matrix, U_{t_0} in (29), the process of (23)–(26) is satisfied and U_{t_0} is drived to the C–NOT gate. The probabilities of $\psi_{0_{33}}$ and $\psi_{0_{44}}$ change from 1 to 0. For the $\psi_{0_{34}}$ and $\psi_{0_{43}}$ these trends are from 0 to 1, and the probabilities of other elements of identity matrix, U_{t_0}, return to their initial values after 1.68 a.u..

In Figs. 3(a)–3(d) there is a clear trend of changing the probabilities, and their evolutions happen in the same time. When the designed control laws of (37) are implemented to columns of U_{t_0}, the columns from left to right are considered as $|00\rangle$, $|01\rangle$, $|10\rangle$ and $|11\rangle$, respectively. At the same time with the same group of control parameters, i.e., $K_1 = 47.5$, $K_3 = 21.7$ and $K_4 = 32.4$, during 4 steps the columns are achieved to, $|00\rangle$, $|01\rangle$, $|11\rangle$ and $|10\rangle$, respectively. Considering (24) and (25), each column (state) of unitary time-evolution matrix has the same probability, and the state only changes from pure to pure superposition state, therefore, during steps 2 and 3 of evolution the probabilities remain unchanged.

The results of correlational analysis are shown in Fig. 4, where the total Fidelity of the C–NOT gate preparation for different control parameters are compared. The Fidelity in this paper is defined as follows in (39). It interprets the proximity between the initial and desired state, i.e., how close the initial state can reach to the target state during the evolution:

$$F(\psi_{\rm f},\ \psi_0) = |\langle\psi_0|\psi_{\rm f}\rangle|. \tag{39}$$

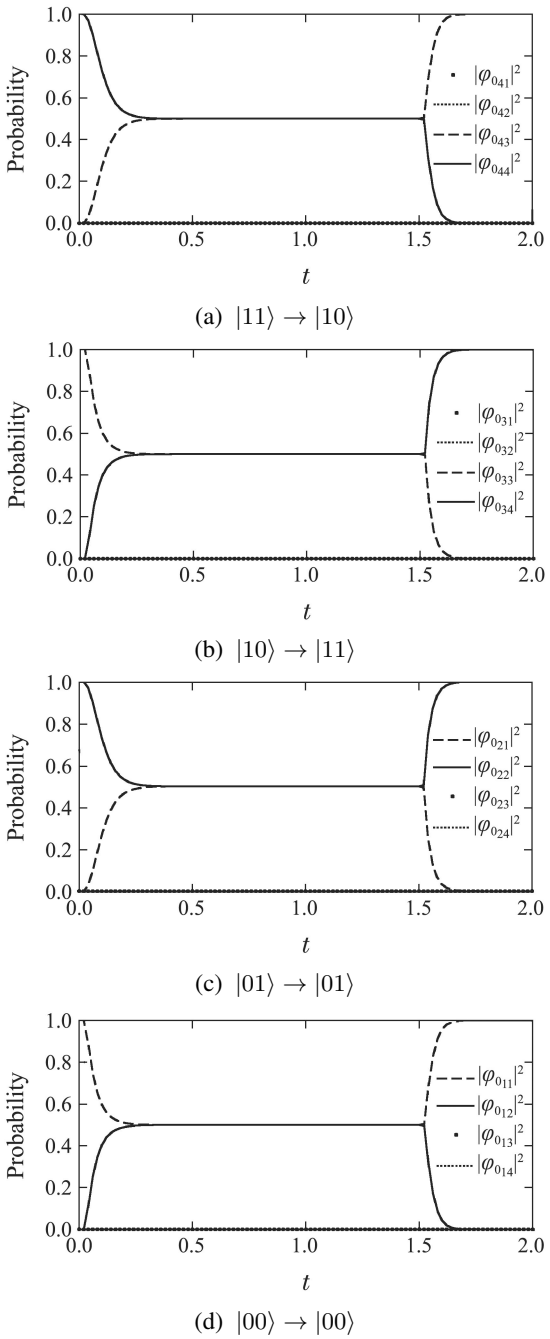

Fig. 3 The probability evolution of each element of U_{t_0} for different initial states as the 1st to 4th columns

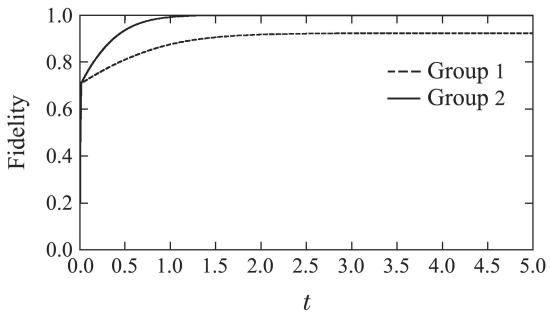

Fig. 4 The total Fidelity of preparing the C–NOT gate when we use the Lyapunov control method with group 1 of control parameters $K_1 = 9$, $K_3 = 7$ and $K_4 = 6$, comparing with the group 2 of control parameters, i.e., $K_1 = 47.5$, $K_3 = 21.7$ and $K_4 = 32.4$

Table 1 provides the results obtained from analyzing the Fidelity for different control parameters. It can be seen that, for $K_1 = 47.5$, $K_3 = 21.7$ and $K_4 = 32.4$ the Fidelity achieves 1 in 1.68 a.u., but when the control parameters are selected as $K_1 = 9$, $K_3 = 7$, and $K_4 = 6$, then the Fidelity maximally gets the value of 0.9197 in 2.91 a.u.. It is because, when the designed control laws are implemented to the system, the deviation around the fixed axis becomes less, and consequently it maximize the Fidelity of the system.

Table 1 The total Fidelity and time for different control parameters, while preparing the C–NOT gate

Control parameters	Maximum Fidelity	Time
Group 1:		
$K_1=9$, $K_3=7$, $K_4=6$	0.9197	2.91
Group 2:		
$K_1=47.5$, $K_3=21.7$, $K_4=32.4$	1	1.68

6 Conclusion

This paper was undertaken to prepare the C–NOT gate by designing the control laws based on the Lyapunov control method and evaluate them in 4 decomposed steps. One of the more significant findings to emerge from this study is that by implementing the designed control laws on each step of evolution, the rotations have less deviations around the fixed axis which brings the higher Fidelity of the system in a short time.

Taken together the present study confirms previous findings about preparing 2 qubit quantum gates and contributes additional evidence that suggests using the Lyapunov control method to design the proper control laws for quantum gate preparation.

References:

[1] SCHMIDT-KALER F, Realization of the Cirac-Zoller controlled-NOT quantum gate. *Nature*, 2003, 422(6930): 408 – 411.

[2] PLANTENBERG J H. Demonstration of controlled-NOT quantum gates on a pair of superconducting quantum bits. *Nature*, 2007, 447(7146): 836 – 839.

[3] BRUSS D. Quantum computing with controlled-NOT and few qubits. *Philosophical Transactions: Mathematical, Physical and Engineering Sciences,* 1997, 355(1733) : 2259 – 2266.

[4] NIELSON L. *Quantum Computation and Quantum Information.* Cambridge: Cambridge University Press, 2010.

[5] PETTA J R. Coherent manipulation of coupled electron spins in semiconductor quantum dots. *Science*, 2005, 309(5744): 2180 – 2184.

[6] EFROS A L. Origin and control of blinking in quantum dots. *Nature Nanotechnology*, 2016, 11(8): 661 – 671.

[7] TAYLOR J M. Relaxation, dephasing, and quantum control of electron spins in double quantum dots. *Physical Review B*, 2007, 76(3): 035315-17.

[8] AWSCHALOM D D, LOSS D. *Semiconductor Spintronics and Quantum Computation.* Berlin: Springer Science and Business Media, 2013.

[9] AWSCHALOM D D. Challenges for semiconductor spintronics. *Nature Physics*, 2007, 3(3): 153 – 159.

[10] BURKARD G. Coupled quantum dots as quantum gates. *Physical Review B*, 1999, 59(3): 2070 – 2078.

[11] LI R. Controllable exchange coupling between two singlet-triplet qubits. *Physical Review B*, 2012, 86(20): 205306-8.

[12] LOSS D. Quantum computation with quantum dots. *Physical Review A*, 1998, 57(1): 120 – 126.

[13] KLINOVAJA J. Exchange-based CNOT gates for singlet-triplet qubits with spin-orbit interaction. *Physical Review B*, 2012, 86(8): 085423-8.

[14] GELLER M R. Quantum logic with weakly coupled qubits. *Physical Review A*, 2010, 81(1): 012320-5.

[15] SCHMIDT-KALER F. Realization of the Cirac-zoller controlled-NOT quantum gate. *Nature*, 2003, 422(6930): 408 – 411.

[16] TANAMOTO T. Efficient purification protocols using iSWAP gates in solid-state qubits. *Physical Review A*, 2008, 78(6): 062313-10.

[17] GHOSH J. Controlled-not gate with weakly coupled qubits: dependence of Fidelity on the form of interaction. *Physical Review A*, 2010, 81(5): 052340-6.

[18] PLESCH M. Quantum-state preparation with universal gate decompositions. *Physical Review A*, 2011, 83(3): 032302-5.

[19] HOU R C. Realization of quantum gates by Lyapunov control. *Physics Letters A*, 2014, 378(9): 699 – 704.

[20] SKLARZ S E. Quantum computation via local control theory: Direct sum vs. direct product Hilbert spaces. *Chemical Physics*, 2006, 322(1/2): 87 – 97.

[21] KUANG S, CONG S. Lyapunov control methods of closed quantum systems. *Automatica*, 2008, 44(1): 98 – 108.

[22] WANG X. Analysis of Lyapunov method for control of quantum states. *IEEE Transactions on Automatic Control*, 2010, 55(10): 2259 – 2270.

[23] WANG W, WANG L C. Lyapunov control on quantum open systems in decoherence-free subspaces. *Physical Review A*, 2010, 82(3): 034308.

[24] WEN J, CONG S. Preparation of quantum gates for open quantum systems by lyapunov control method. *Open Systems and Information Dynamics*, 2016, 23(1): 1650005-18.

[25] LOSS D. Quantum computation with quantum dots. *Physical Review A*, 1998, 57(1): 120 – 126.

[26] CONG S. *Control of Quantum Systems: Theory and Methods.* Singepore: John Wiley and Sons, 2014.

[27] ASHCROFT N W. *Solid State Physics*. Singepore: Saunders College, 1976, 32: 584.

作者简介:

NOURALLAH Ghaeminezhad 博士, 目前研究方向为量子系统控制、量子门的制备、开放量子系统的反馈控制, E-mail: ghaemi@mail.ustc.edu.cn;

丛 爽 教授, 博士生导师, 目前研究方向为量子系统及其控制、先进控制系统及运动控制, E-mail: scong@ustc.edu.cn;

双 丰 教授, 博士, 目前研究方向为量子系统控制、量子测量、多维力传感器、力反馈控制, E-mail: fshuang@iim.ac.cn.